



**ARTICLE**

## Experimental Synthesis of Polyacrylic-Type Superabsorbent Polymer and Analysis of Its Internal Curing Performances

Jin Yang<sup>1,2</sup>, Wen Liang<sup>1</sup>, Xingyang He<sup>1,2,\*</sup>, Ying Su<sup>1,2</sup>, Fulong Wang<sup>1</sup>, Tie Wang<sup>1</sup> and Jianxiang Huang<sup>1</sup>

<sup>1</sup>School of Civil Engineering, Architecture and Environment, Hubei University of Technology, Wuhan, 430068, China

<sup>2</sup>Building Waterproof Engineering and Technology Research Center of Hubei Province, Hubei University of Technology, Wuhan, 430068, China

\*Corresponding Author: Xingyang He. Email: hexycn@163.com

Received: 08 July 2021 Accepted: 22 September 2021

### ABSTRACT

A solution polymerization method has been used to synthesize a polyacrylic-type superabsorbent polymer (SAP). The influence of various influential factors, such as the temperature, neutralization degree, cross-linking agent, and initiator, on the water absorption capacity of SAP has been investigated. The results show that the absorption can display a non-monotonic behavior depending on the synthesis conditions. The absorption can also change according to the pH, ion types and ion concentration. As the pH value increases, the water absorption capacity decreases significantly. It also decreases if the Na<sup>+</sup> concentration becomes higher and becomes particularly low in solutions containing Mg<sup>2+</sup>. With the addition of SAP, the compressive strength of cement mortar decreases; the internal relative humidity can be maintained at 96% within 200 hours; and autogenous shrinkage can be reduced by nearly 69%.

### KEYWORDS

Superabsorbent polymer; synthesis; internal relative humidity; internal curing

## 1 Introduction

High-performance and high-strength cement-based materials [1,2] have been widely used in large-scale projects such as ultra-long and large-span structures and ultra-high-rise buildings, and continue to expand their applications to complex environments, such as oceans, underground and high altitudes. Low water-binder ratio is the main technical means for cement-based materials to achieve high strength and high durability. It is generally believed that the durability of high-performance cement-based materials is great, but a low water-to-binder ratio will lead to poor crack resistance of high-performance cement-based materials. If cracks occur, the high durability of this material cannot be guaranteed. Autogenous shrinkage and self-desiccation due to water consumption [3] are the main reasons for the early cracking of cement-based materials.

Superabsorbent polymer (SAP) is a typical internal curing agent to prevent cracking [4,5]. SAP has been widely used in various fields such as agriculture, horticulture and drug delivery systems in the past 30 years. SAP [6] is a polymer containing strong hydrophilic groups such as carboxyl (-COOH) and hydroxyl (-OH) [7,8], which can form hydrogen bonds with water molecules. SAP can be used to improve the relative



humidity inside the cement paste and shrinkage performance [9–11]. At present, there is a lot of work on absorption of SAP under different influencing factors. The performances of SAP under different conditions may be quite different from each other, so that it is particularly important to conduct a comprehensive study with different synthesis factors [12–14]. Therefore, it is necessary to study water absorption of SAP in different solution and evaluate its internal curing performances on in cement based materials.

The solution polymerization method was used in present work to prepare polyacrylic-type SAP. The influence of temperature, neutralization degree, cross-linking agent and initiator dosage on SAP water absorption performance was also investigated. In addition, the internal relative humidity, compressive strength and auto-shrinkage tests are also used to evaluate the impact of its internal performance in the concrete.

## 2 Raw Materials and Methods

### 2.1 Raw Materials

- 1) Acrylic acid (AA): colorless, pungent smell,  $C_3H_4O_2$  solution;
- 2) Sodium hydroxide: NaOH, 99% of white uniform flaky solid;
- 3) Crosslinking agent: NMBA, white powder, no pungent smell;
- 4) Initiator: KPS, white, flake particles, chemical formula is  $K_2S_2O_8$ .

### 2.2 Synthesis of Polyacrylic-Type Superabsorbent Polymer

The water bath was filled with water, the synthesis temperature (50–70°C) was set, and a 250 mL dry beaker was used to get a certain amount of deionized water. The NaOH solid was weighed and mixed with deionized water. The acrylic acid solution was weighed into a beaker, the NaOH solution was added dropwise into the acrylic acid solution while stirring, and weighing paper was used to weigh NMBA and potassium persulfate into the solution. Solution was stirred in a constant temperature water bath for several hours to form a gel. The polymerized gel was dried and crushed to form SAP powder with particle size of 300 and 450 microns. The water absorption capacity of prepared polyacrylic-type was determined in tape water and fresh cement paste. Absorption capacity of SAP in tape water was more than 100 g/g, and the capacity in fresh cement paste was about 10 g/g determined by fluidity method.

### 2.3 Mixture Proportion

The prepared superabsorbent polymer was added to cement mortar to explore its internal curing performances, including compressive strength, autogenous shrinkage and internal relative humidity. First, the additional water is the amount of theoretically introduced water required to obtain the maximum degree of hydration, 0.063 g of water per 1 g of cement. After the addition of SAP powder and additional water, it should not have an obvious impact on the workability of the cement mortar. The additional water introduced in the cement mortar should be theoretically absorbed completely by the absorbent polymer. Mixture proportion of mortar with SAP was presented in [Table 1](#).

**Table 1:** Mixture proportion of mortar with SAP

	Cement	Sand	SAP	Water	The amount of additional water entrained
Control	1	1	0	0.35	0
SAP-AA	1	1	0.0063	0.35	0.063

## 2.4 Testing Method

### 2.4.1 Determination of Water Absorption Rate

Using an analytical balance, a small amount of SAP mass  $m_1$  whose unit was “g” was taken after grinding and sieving, the tea bag was moistened in the solution, and the SAP was put into the wet tea bag. The mass was weighed and recorded the  $m_2$  (g). It was put in the beaker with test solution, and taken out after 4 min and wiped the surface of the tea bag with a pre-moistened towel to ensure that there was no residual moisture in the SAP. After weighing the mass  $m_3$  (g), its final water absorption rate would be calculated by Eq. (1).

$$A_t = \frac{m_3 - m_2}{m_1} \quad (1)$$

### 2.4.2 Determination of Absorption Rate in Salt Containing Solution

0.2 mol/L, 0.4 mol/L and 0.6 mol/L NaCl solution, 0.2 mol/L  $MgCl_2$  solution and 0.2 mol/L  $AlCl_3$  solution was prepared, respectively. The absorption rate of SAP in above solution was determined. The determination method was the same as Section 2.4.1.

### 2.4.3 Particle Size Distribution Test

A laser particle size analyzer was used in this study. Alcohol was used as the dispersion medium for laser particle size test, because of the water absorption characteristics of superabsorbent polymer [15]. First, 0.5 g of different types of superabsorbent polymer was taken, and ultrasonic waves were used to make the sample fully dispersed in the alcohol medium.

### 2.4.4 Fourier Transform Infrared Spectroscopy

The infrared transmission spectrum of SAP was tested with fourier infrared spectrometer. Before the test, the samples were dried in a drying oven at 50°C for 24 h and passed through a sieve of 75  $\mu m$ . In order to obtain a clear spectrum, 1 mg of pure slurry powder and 100 mg of KBr were mixed and extruded into circular flakes. The spectrum test range was from 400  $cm^{-1}$  to 4000  $cm^{-1}$ , and the band intensity was expressed by the transmittance.

### 2.4.5 SEM Test

Quanta 450 FEG SEM with an acceleration voltage of 15 kV was used to examine the microstructure of the SAP modified mortars. Samples were coated with gold to gain the electric conductivity. Morphology of cement mortars at 28 days were examined by SEM.

### 2.4.6 Compressive Strength Test

Specimens were prepared with the size of 40 mm  $\times$  40 mm  $\times$  40 mm according to GB/T 17671 [16] using plastic molds, and then cured in standard condition at 23°C and RH > 95%. The DYE-300A digital pressure tester produced by North Jianyi Technology Co., Ltd., Beijing, China was used for the test of compressive strength. Compressive loading rate was kept at 2.4 KN/s.

### 2.4.7 Autogenous Shrinkage Test

Specimens of 40 mm  $\times$  40 mm  $\times$  160 mm were prepared in standard curing room for 24 h. The demoulded specimens were sealed with plastic film so that the specimens did not exchange moisture with the external environment. Then it was placed firmly on the 32-channel automatic concrete shrinkage and dilatometer, and the ambient temperature was controlled at (20  $\pm$  2)°C. The length change of the specimen was measured by the electronic displacement probe on the cantilever, and the electronic probe touched the top of the specimen. The data was automatically collected by the microcomputer for 7 days.

#### 2.4.8 Internal Relative Humidity Test

A HKT-XY type 8-channel precision temperature and humidity inspection recorder was adopted. Humidity test was ranged from 0% to 100% RH. The test probe was put into the plastic tube using polyethylene tape. The temperature was kept at 20°C and the data was monitored every 2 minutes for 7 days.

### 3 Results and Discussion

#### 3.1 Effect of Synthesis Condition on Liquid Absorption Performance

##### 3.1.1 Effect of Synthesis Temperature

Fig. 1 shows the effect of different temperature on the water absorption rate of SAP in deionized water [17]. It can be studied that the water absorption rate of SAP increases as the temperature increases from 50°C to 65°C, and then decreases after 65°C. The highest water absorption rate reached 120 g/g at 65°C. As mentioned in Raju et al. [18], if the temperature is low enough, the gel cannot be formed. The reason is that the reaction temperature is too low and the initiator reaction rate is reduced. Within a certain period, AA monomer cannot be effectively converted into a cross-linked structure and part of the polymer chain is water-soluble, it will dissolve in contact with water and cannot form a complete chain, resulting in a low water absorption rate of the synthesized SAP. Conversely, the initiator will decompose too fast, if the temperature is too high, causing the reaction monomer to burst out of the reaction flask, and the reaction process cannot be controlled. When reaction temperature is too high, the reaction rate of the system is too fast, causing the molecular chain between the cross-linked structures of the reaction product to be too short, thereby reducing the water absorption performance of SAP.

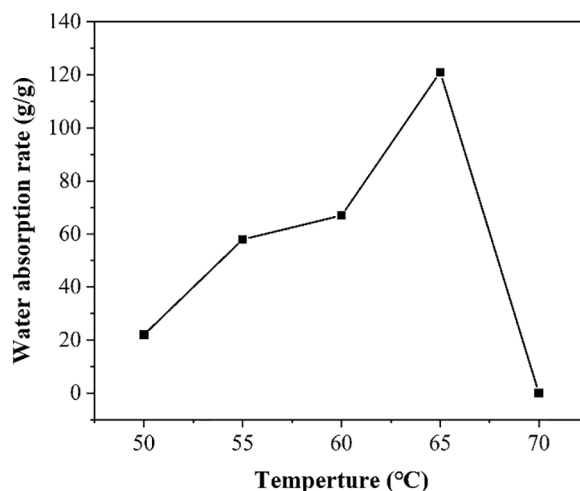


**Figure 1:** Water absorption rate of SAP under the influence of different synthesis temperature

##### 3.1.2 Effect of Neutralization Degree

Fig. 2 shows the water absorption rate of SAP under the influence of different neutralization degrees. It can be seen that as the neutralization degree increases, water absorption rate rises first and falls then, reaching a peak at 70%. When the degree of neutralization is low, the concentration of AA monomer and the activity of AA monomer is very high, which will cause the polymerization speed of the reaction system to be very fast. The self-polymerization reaction is easy to occur, easily forming a polymer with excessively high cross-linking, thereby resulting in a decrease in the water absorption rate of the synthesized SAP in deionized water. It is worth noting that the neutralization degree of the system should not be too high which will cause the amount of monomer in the system to be too low, resulting in a decrease in the reaction rate.

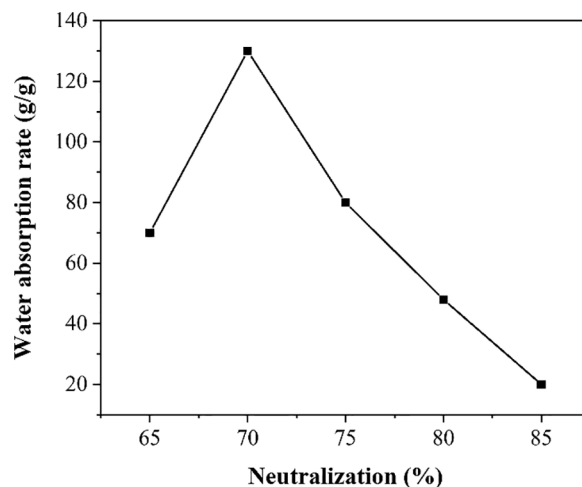


**Figure 2:** Water absorption rate of SAP under the influence of different neutralization degrees

### 3.1.3 Effect of Cross-Linking Agent

Fig. 3 shows the influence of different crosslinking agent dosages on the water absorption rate of SAP. It can be seen that when the crosslinking agent content for the mass percentage of acrylic acid gradually increases, the water absorption rate of SAP shows a trend of increasing first and decreasing later. The reason may be attributed to the quality of the crosslinking agent. When the cross-linking agent content is too low, the reaction system is not suitable to form an ideal three-dimensional cross-linking network. And a large part of the monomers have not successfully cross-linked each other, resulting in a significant decrease in water absorption rate; when the cross-linking agent content for the mass percentage of acrylic acid is too high, the cross-linking density is too large. Although the molecular chain can expand smoothly, the network pores among molecules are too small, which is not conducive to the entry of water molecules, thus resulting in a decreasing trend in the water absorption rate of SAP.

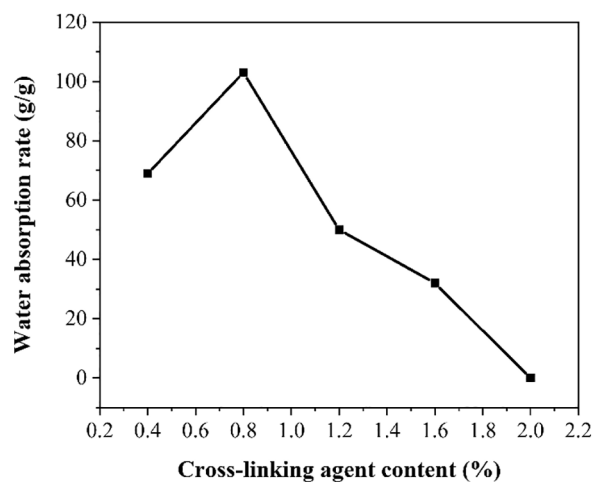


**Figure 3:** Water absorption rate of SAP under the influence of different cross-linking agent content for the mass percentage of acrylic acid

### 3.1.4 Effect of Initiator Agent Content

Fig. 4 shows the change of water absorption rate of SAP under different initiator content. The water absorption rate reached the highest value, when the initiator content for the mass percentage of acrylic acid is 1.5%. As the amount of initiator increases, it shows a trend of increase first and decrease later. When the amount of initiator is too small, there are too few active centers in the system during synthesis, reducing the reaction rate, and the cross-linking of SAP's three-dimensional cross-linking network. When initiator agent content for the mass percentage of acrylic acid is too low, the water absorption rate will be reduced; when the initiator agent content for the mass percentage of acrylic acid is too large, the reaction system will polymerize too quickly and increase the activity. At this time, the molecular chain on the AA would tend to be short, and the molecular weight will reduce, resulting in a decrease in the water absorption rate.

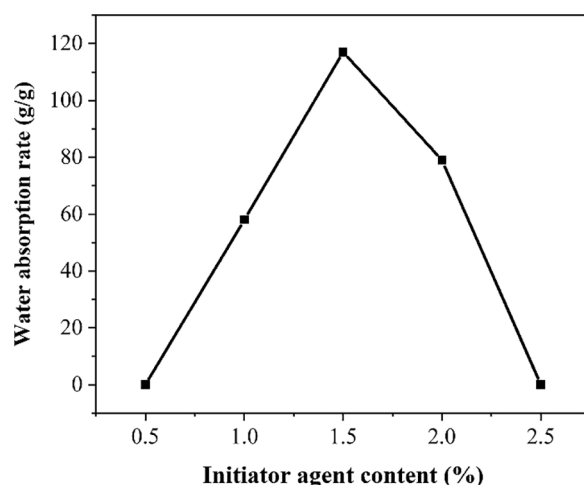


**Figure 4:** Water absorption rate of SAP under different initiator agent content for the mass percentage of acrylic acid

## 3.2 Absorption Rate in Inorganic Salt Solution

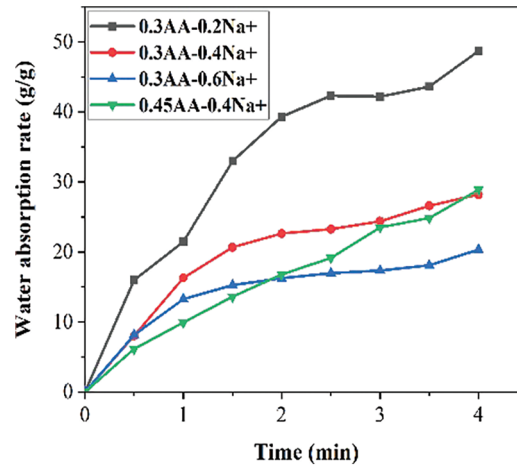
### 3.2.1 Effect of Different Ion Concentration

Fig. 5 shows the water absorption change law of SAP in solution with different ion concentrations. It was observed that the water absorption rate of SAP was 45 g/g, when the  $\text{Na}^+$  concentration was 0.2 mol/L. When the  $\text{Na}^+$  concentration was increased to 0.6 mol/L, its water absorption rate was only 20 g/g. The reason for this phenomenon may be that the carboxyl group on the SAP undergoes a complex reaction with the cation in the solution, which affects the hydrophilic group of the SAP. In addition, the ions in the salt solution will change the penetration between the SAP and the ions in the solution. The ion shielding effect will weaken the electrostatic repulsion among the anions, resulting in a decrease in the water absorption rate. Finally, the plots in Fig. 5 explain that the small particle size absorbs quickly, but as time goes by, the two particle sizes are basically the same.

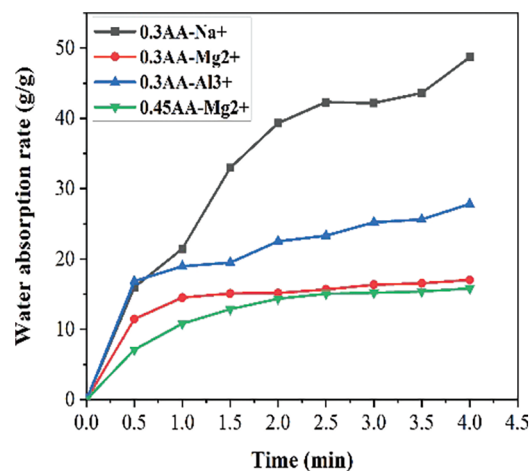
### 3.2.2 Effect of Different Ion Types

Fig. 6 shows the water absorption rate changes of SAP in solution with different ion types. As mentioned above, its water absorption rate in deionized water is about 120 g/g. From the figure, it can be observed that water absorption rate in the 0.2 mol/L  $\text{Al}^{3+}$  and  $\text{Mg}^{2+}$  solution is much lower than that in deionized water, as the valence state of the ions in the solution increases. The water absorption rate in 0.2 mol/L  $\text{Mg}^{2+}$  solution is only 17 g/g, which is 66% lower than  $\text{Na}^+$  solution. The water absorption rate in 0.2 mol/L  $\text{Al}^{3+}$  solution is

28 g/g, which is 50% lower than  $\text{Na}^+$  solution. This phenomenon occurs because the valence state of the cation determines the number of hydroxyl groups consumed to form a complex with the anion on the SAP. High-valent cations will reduce anions to varying degrees, and the electrostatic repulsion among them will also decrease, so that water absorption rate becomes lower. In addition, as the sodium ion concentration increases, its water absorption rate gradually decreases. The water absorption rate of SAP with a particle size of 0.3 mm and 0.45 mm is also similar, which is in line with the above conclusion.



**Figure 5:** The water absorption curve of SAP in solution with different ion concentrations



**Figure 6:** Water absorption curve of SAP in solution with different ion types

### 3.2.3 Effect of Different pH Values

As shown in Fig. 7, the water absorption rate of SAP with different particle sizes in pH = 7 and pH = 13 solution are different. It can be seen that water absorption rate in pH = 7 solution is much higher than that in pH = 13 solution. It was found that SAP with a particle size of 0.3 mm has the higher water absorption rate. In the pH = 13 solution, the SAP with a particle size of 0.3 mm and 0.45 mm only absorbs 27 g/g and 23 g/g alkaline solution. When deionized water is changed to alkaline solution, it will

have strong ion shielding effect on its molecular chains and will also affect the osmotic pressure in it, especially for ionic SAP type, which is more sensitive to ions in the solution.

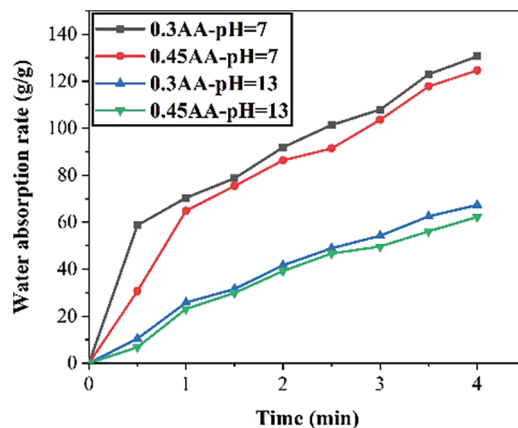


**Figure 7:** Water absorption curve of SAP in solution with different pH values

### 3.3 Physical and Chemical Characterization

#### 3.3.1 Particle Size Distribution

Fig. 8a is the particle size distribution of SAP used in present work. It can be seen that median particle size of SAP is about 300  $\mu\text{m}$  and 450  $\mu\text{m}$ . Generally speaking, smaller particle size of the SAP has larger contact area with water, its early water absorption rate will be higher and faster. However, the water absorption rate of the polymer with a particle size of 300 microns is not necessarily higher than 450 microns. It also depends on the specific water absorption time. The final water absorption rate of SAP with larger particle size would be theoretically close to that with small particle size.

#### 3.3.2 FTIR

Fig. 8b shows the FTIR of synthesized SAP. From the FTIR curve, we can see that  $3440\text{ cm}^{-1}$  is the stretching vibration peak of OH in  $-\text{COOH}$  and is related to the stretching vibration of the NH bond,  $2950\text{ cm}^{-1}$  is the CH symmetric stretching vibration peak, and  $1650\text{ cm}^{-1}$  is C=O stretching vibration peak in  $-\text{COOH}$ . Several characteristic peaks in the figure are consistent with the peaks of synthetic substances, indicating that SAP is synthesized after related processing.

#### 3.3.3 Scanning Electron Microscope

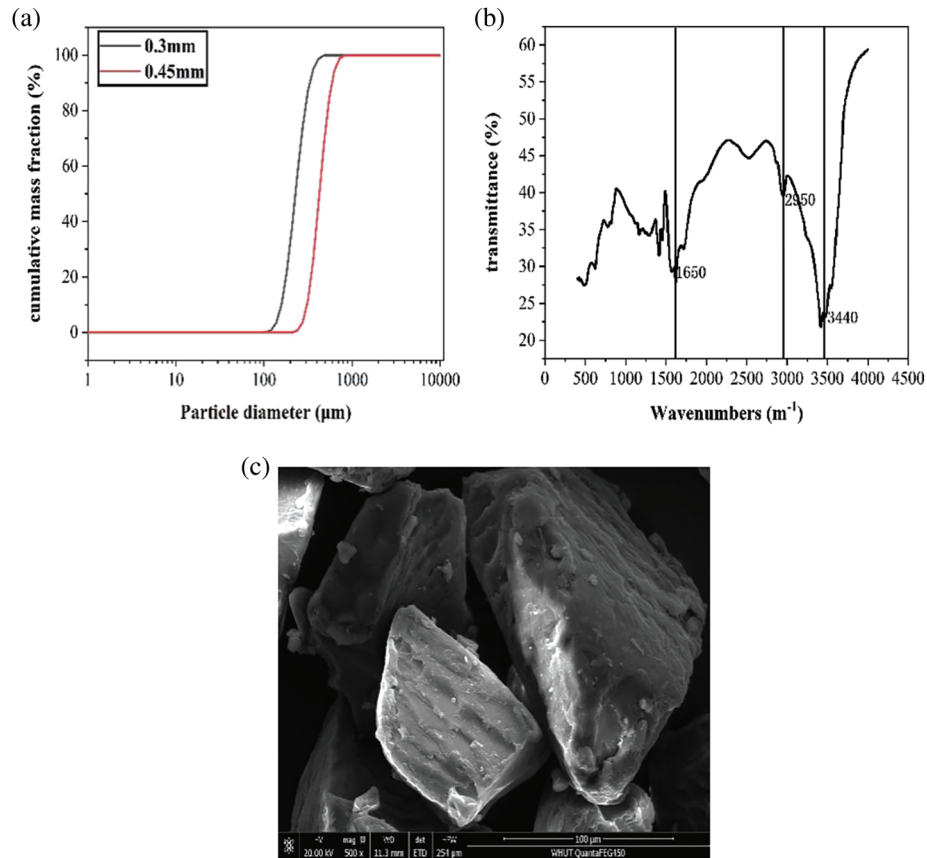
Fig. 8c shows the morphology of crushed SAP powder. It can be seen from the figure that SAP are irregular particles with multiple folds and stripes obviously appearing on the surface. The shape of the particles is both irregular and multi-lobed. After grinding, there are a lot of chips on the periphery. This may be due to the low mechanical strength of SAP.

### 3.4 Performances and Microstructure of Cement Mortar with Poly(AA) SAP

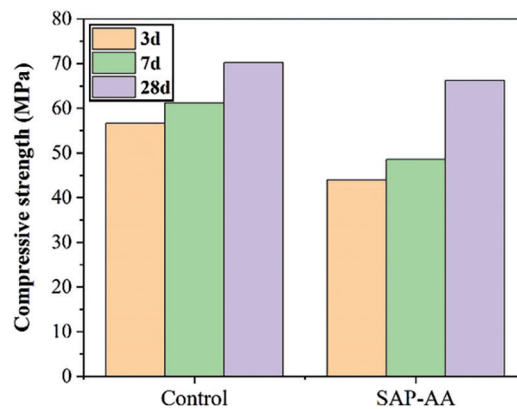
#### 3.4.1 Compressive Strength

Fig. 9 shows the influence of poly(AA) SAP (SAP-AA) on the compressive strength of mortar at different curing ages. It was found that strength of the mortar was reduced after the addition of SAP-AA. At 3 d, the strength of the SAP-AA sample was 43 MPa, which was 12 MPa lower than that of the control group at the same age. The negative effect of SAP-AA on the strength of mortar was mainly before 7 d. At 28 d, the strength of the SAP-AA sample was 65 MPa, which was close to that of the control group. This should be attributed to the effect of internal curing which increases the degree of

hydration around SAP-AA and promotes the strength development in the later stage. It improves the degree of hydration by providing internal water, at the same time creates macroscopic voids in the matrix to increase the porosity of concrete. These conflicting effects depend on the water-cement ratio, SAP chemical composition and SAP particle size, etc.



**Figure 8:** Particle size distribution (a) FTIR (b) and SEM (c) of SAP



**Figure 9:** Compressive strength of cement mortar with SAP at different ages

### 3.4.2 Internal Relative Humidity

Fig. 10 shows the change of the relative humidity inside the specimens with SAP-AA under the sealed condition. It can be seen from the figure that compared with the control group, the addition of SAP can significantly delay the decrease of relative humidity inside the specimen. Within 200 hours, the internal relative humidity of the control maintains at 92% at the beginning, and it decreases to 87% at 7 days, whereas the internal relative humidity of the SAP-AA samples can be maintained at 96%, which is almost unchanged. This is because under the action of the humidity gradient, SAP-AA will continuously release water to maintain the internal relative humidity of the cement-based material [19]. In addition, as the cement hydration progresses, the internal water is gradually consumed, causing the concentration to increase in the pore solution. According to the law of Van Hoff, the difference in solution concentration will produce osmotic pressure. Under its action, the water in SAP will be continuously released and added into the cement paste to keep its internal relative humidity.

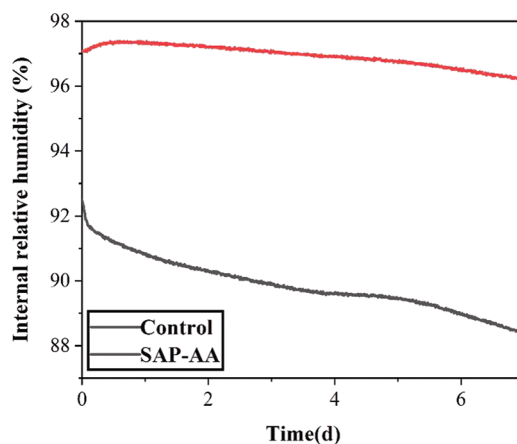


**Figure 10:** Internal relative humidity of cement mortar with and without SAP

### 3.4.3 Autogenous Shrinkage

Fig. 11 shows the change in autogenous shrinkage of samples with SAP-AA within 7 days. The shrinkage value of the control group at 7 days is around 0.14%, while the change in shrinkage of the SAP-AA sample is only 0.04%. Compared with the control group, the autogenous shrinkage of the SAP-AA sample group was reduced by nearly 70%. The reason for SAP's excellent effect of reducing autogenous shrinkage is that the incorporation of SAP-AA introduces additional internal curing water [20]. The introduction of additional internal curing water [21] will cause the total water-cement ratio to increase, the autogenous shrinkage of the mortar decreases [22]. In addition, with the progress of cement hydration, the incorporation of SAP-AA will significantly delay the self-desiccation, when the relative humidity inside the cement-based material decreases. Internal humidity of the cement-based material mixed with SAP-AA is much higher than that of the control group at the same age. As the relative humidity inside the specimen decreases, the internal curing water stored in the SAP would be gradually released into the cement-based material [23–25], which can effectively reduce the autogenous shrinkage of the cement based materials.

Generally, polyacrylic-type superabsorbent polymer was prepared considering different synthesis temperature, neutralization degree, crosslinking agent and initiator content. However, the influence of different monomer types was not considered in present work. At the same time, compared with the existing reports, the water absorption capacity of SAP synthesized in this work is not particularly high, which is also the area that needs to be further improved in the future work.

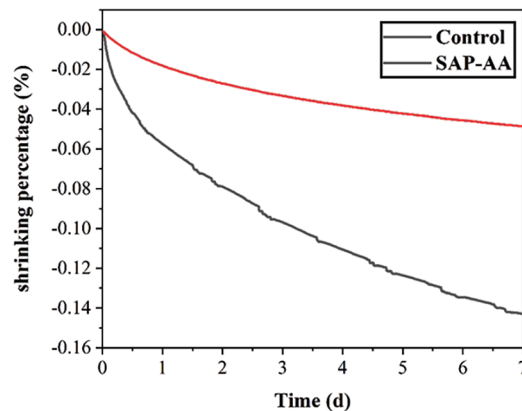


**Figure 11:** Autogenous shrinkage of samples with and without SAP

#### 4 Conclusion

In this work, an aqueous solution polymerization method is used to synthesize acrylic-type superabsorbent polymer. It is characterized by SEM, FTIR and particle size analysis. The tea bag method is used to analyze the change of water absorption capacity in different types of solution. Relative humidity, autogenous shrinkage and compressive strength were conducted to explore the influence of synthesized SAP on the performances of cement mortar.

1) The best synthesis conditions for SAP in present work: neutralization degree 70%, synthesis temperature 65°C, crosslinking agent content 0.8%, initiator agent content 1.5%. The water absorption rate reaches up to 120–140 g/g, and the salt absorption rate in the salt solution is about 48 g/g.

2) In different solution conditions, it is concluded that the water absorption rate in an alkaline environment will be greatly reduced. As the ion concentration increases, the water absorption rate of the SAP will gradually decrease. As the cation valence increases, water absorption capacity of SAP will reduce more than 50%.

3) Autogenous shrinkage of the sample mixed with SAP was reduced by nearly 70%, compared with that of control group without acrylic-type SAP.

4) Compared to the control group with an internal relative humidity of only 87%, the internal relative humidity of specimen with SAP was kept at 96% within 200 h.

**Funding Statement:** The authors would like to acknowledge the National Natural Science Foundation of China (51902095).

**Conflicts of Interest:** The authors declare that they have no conflicts of interest to report regarding the present study.

#### References

- Liu, C., Wu, Y., Gao, Y., Tang, Z. (2021). Experimental and numerical analysis of high-strength concrete beams including steel fibers and large-particle recycled coarse aggregates. *Fluid Dynamics & Materials Processing*, 17(5), 947–958. DOI 10.32604/fdmp.2021.016283.
- Liu, C., Xu, J., Gu, Y., Shi, R. (2021). Experimental study on the axial compression behavior of short columns of steel-fiber-reinforced recycled aggregate concrete. *Fluid Dynamics & Materials Processing*, 17(5), 1129–1142. DOI 10.32604/fdmp.2021.017376.
- Wang, Y., Wang, H., Yang, L., Qian, L. (2021). Coupled effects of heat and moisture of early-age concrete. *Fluid Dynamics & Materials Processing*, 17, 845–857. DOI 10.32604/fdmp.2021.015961.

4. Soo, K. J., Hyun, K. D., Suk, L. Y. (2021). The influence of monomer composition and surface-cross-linking condition on biodegradation and gel strength of super absorbent polymer. *Polymers*, 13(4), 1–2. DOI 10.3390/polym13040663.
5. Wu, C. C., Srivatsan, R., Alexandra, P., Jose, A. (2021). Dewatering of super absorbent polymers: Alternatives to thermal desorption by liquid phase extraction using dimethyl ether. *Resources, Conservation and Recycling*, 171, 105641. DOI 10.1016/j.resconrec.2021.105641.
6. Snoeck, D., Goethals, W., Hovind, J., Trtik, P., van Mullem, T. et al. (2021). Internal curing of cement pastes by means of superabsorbent polymers visualized by neutron tomography. *Cement and Concrete Research*, 147(17), 106528. DOI 10.1016/j.cemconres.2021.106528.
7. Xi, J. J., Zhang, P. P. (2021). Application of super absorbent polymer in the research of water-retaining and slow-release fertilizer. *IOP Conference Series: Earth and Environmental Science*, 651(4), 1–2.
8. Liang, Z. R., Cai, X. N., Hu, H. Y., Zhang, Y. J. (2021). Synthesis of starch-based super absorbent polymer with high agglomeration and wettability for applying in road dust suppression. *International Journal of Biological Macromolecules*, 183, 1–2. DOI 10.1016/j.ijbiomac.2021.05.015.
9. Mousavi, S. S., Guizani, L., Bhojaraju, C., Ouellet-Plamondon, C. M. (2021). Application of superabsorbent polymer as self-healing agent in self-consolidating concrete for mitigating precracking phenomenon at the rebar-concrete interface. *Journal of Materials in Civil Engineering*, 33(10), 04021269. DOI 10.1061/(ASCE)MT.1943-5533.0003881.
10. Chidiac, S. E., Mihaljevic, S. N., Krachkovskiy, S. A., Goward, G. R. (2021). Efficiency measure of SAP as internal curing for cement using NMR & MRI. *Construction and Building Materials*, 278(2), 122365. DOI 10.1016/j.conbuildmat.2021.122365.
11. Mousavi, S. S., Ouellet-Plamondon, C. M., Guizani, L., Bhojaraju, C., Brial, V. (2020). On mitigating rebar-concrete interface damages due to the pre-cracking phenomena using superabsorbent polymers. *Construction and Building Materials*, 253, 119181. DOI 10.1016/j.conbuildmat.2020.119181.
12. Yulia, K., Sergey, G., Igor, K. (2021). Evaluation and X-ray tomography analysis of super-absorbent polymer for water management in high salinity mature reservoirs. *Journal of Petroleum Science and Engineering*, 196, 4–6. DOI 10.1016/j.petrol.2020.107998.
13. Yang, Y. H., Wu, J. C., Zhao, S. W. (2021). Effects of long-term super absorbent polymer and organic manure on soil structure and organic carbon distribution in different soil layers. *Soil and Tillage Research*, 206, 4–10. DOI 10.1016/j.still.2020.104781.
14. Tenório Filho, J. R., Mannekens, E., Snoeck, D., de Belie, N. (2019). Investigating the efficiency of ‘in-house’ produced hydrogels as internal curing agents in cement pastes. *2nd International Conference on Sustainable Building Materials*, pp. 37–43. Eindhoven.
15. Tatsuro, N., Yukihiko, O., Harumi, S. (2021). Study of changes in water structure and interactions among water, CH<sub>2</sub> and COO<sup>-</sup> groups during water absorption in acrylic acid-based super absorbent polymers using Raman spectroscopy. *Spectrochimica Acta Part A: Molecular and Biomolecular Spectroscopy*, 250, 4–6. DOI 10.1016/j.saa.2020.119305.
16. Liu, K., Chen, W., Ye, J. H. (2021). Improved fire resistance of cold-formed steel walls by using super absorbent polymers. *Thin-Walled Structures*, 160, 4–5. DOI 10.1016/j.tws.2020.107355.
17. Mazí, H., Surlmelhíndí, B. (2021). Temperature and Ph-sensitive super absorbent polymers based on modified maleic anhydride. *Journal of Chemical Sciences*, 133(1), 4–5. DOI 10.1007/s12039-020-01873-3.
18. Raju, K., Raju, M. (2002). Synthesis and water absorbency of cross linked superabsorbent polymers. *Journal of Applied Polymer Science*, 85(8), 1795–1801. DOI 10.1002/(ISSN)1097-4628.
19. Xie, F. X., Cai, D. P., Lin, J. (2021). Combined compression-shear performance and failure criteria of internally cured concrete with super absorbent polymer. *Construction and Building Materials*, 266, 3–11. DOI 10.1016/j.conbuildmat.2020.120888.
20. Mousavi, S. S., Guizani, L., Bhojaraju, C., Ouellet-Plamondon, C. (2021). The effect of air-entraining admixture and superabsorbent polymer on bond behaviour of steel rebar in pre-cracked and self-healed concrete. *Construction and Building Materials*, 281(9), 122568. DOI 10.1016/j.conbuildmat.2021.122568.

21. Snoeck, D., Jensen, O. M., de Belie, N. (2015). The influence of superabsorbent polymers on the autogenous shrinkage properties of cement pastes with supplementary cementitious materials. *Cement and Concrete Research*, 74, 59–67. DOI 10.1016/j.cemconres.2015.03.020.
22. Zhao, H. T., Ding, J., Huang, Y. Y. (2020). Investigation on sorptivity and capillarity coefficient of mortar and their relationship based on microstructure. *Construction and Building Materials*, 265, 3–9. DOI 10.1016/j.conbuildmat.2020.120332.
23. Yang, J., Wang, F., Liu, Z., Liu, Y., Hu, S. (2019). Early-state water migration characteristics of superabsorbent polymers in cement pastes. *Cement and Concrete Research*, 118(6), 25–37. DOI 10.1016/j.cemconres.2019.02.010.
24. Yang, J., Wang, F. (2019). Influence of assumed absorption capacity of superabsorbent polymers on the microstructure and performance of cement mortars. *Construction and Building Materials*, 204(4), 468–478. DOI 10.1016/j.conbuildmat.2019.01.225.
25. Yang, J., Huang, J., He, X., Su, Y., Oh, S. K. (2020). Shrinkage properties and microstructure of high volume ultrafine phosphorous slag blended cement mortars with superabsorbent polymer. *Journal of Building Engineering*, 29(2), 101121. DOI 10.1016/j.job.2019.101121.